REPORT
doi:10.26443/seismica.v5i2.2716

SEISMICA

CRESCENT Earthquake Dynamic Rupture, Earthquake Cycle, and Tsunami Code Verification Platform

Loïc Bachelot * [1,2], **Fabian Kutschera** [3], **Michael Barall** [4], **Brittany A. Erickson** [5,1], **Eric M. Dunham** [6,7], **Alice-Agnes Gabriel** [3,8], **Ruth Harris** [4], **Shuo Ma** [9], **Amanda M. Thomas** [10], **Wenqiang Zhang** [6]

[1]Department of Earth Sciences, University of Oregon, Eugene, OR, USA, [2]Cascadia Region Earthquake Science Center, Eugene, OR, USA, [3]Institute of Geophysics and Planetary Physics, Scripps Institution of Oceanography, University of California San Diego, La Jolla, CA, USA, [4]USGS Earthquake Science Center, Moffett Field, CA, USA., [5]Department of Computer Science, University of Oregon, Eugene, OR, USA, [6]Department of Geophysics, Stanford University, Stanford, CA, USA, [7] Institute for Computational and Mathematical Engineering, Stanford University, Stanford, CA, USA, [8]Department of Earth and Environmental Sciences, Ludwig-Maximilians-Universität München, Munich, Germany , [9]Department of Earth and Environmental Sciences, San Diego State University, San Diego, CA, USA, [10]Department of Earth and Planetary Sciences, University of California, Davis, CA, USA

Author contributions: *Conceptualization*: LB, FK, MB, BE, EMD, AAG, RH, SM, AMT, WZ. *Methodology*: LB, FK. *Software*: LB. *Validation*: LB, FK, SM, WZ. *Resources*: AMT, AAG. *Writing - Original draft*: LB, FK. *Writing - Review & Editing*: LB, FK, AAG, MB, BE, EMD, RH, AMT. *Visualization*: LB, FK. *Supervision*: LB, AAG. *Funding acquisition*: AMT, AAG.

Abstract Physics-based simulations are critical for understanding natural hazards. The increasing complexity of numerical codes requires benchmark exercises to verify that different computational methods yield consistent results when solving the same governing equations. Here, we present an open-access web platform designed for the verification of earthquake dynamic rupture, seismic cycle, and tsunami simulations. The platform architecture utilizes a modular, serverless backend on Amazon Web Services (AWS) to provide scalable file processing and visualization. A lightweight static web application provides a secure interface for uploading and managing results, while the browser-based data visualization enables interactive analysis of time series and surface grid data. By using structured JavaScript Object Notation (JSON) text files to define benchmark structures, the system remains fully extensible, allowing the addition of new scenarios without modifying the underlying software logic. The platform hosts the "The Tsunami Problem Versions" (TTPV) 1 & 2, two benchmarks for 3D fully coupled earthquake dynamic rupture and tsunami generation, and provides a framework for earthquake cycle models. This community resource aims to build trust in numerical simulations and facilitate long-term collaborative code verification as modeling software continues to evolve.

Production Editor:
Gareth Funning
Handling Editor:
Marlon Ramos
Copy & Layout Editor:
Anna Ledeczi

Received:
27 February 2026
Accepted:
24 July 2026
Published:
12 August 2026

1 Introduction

Large earthquakes and tsunamis are among the most destructive natural hazards on Earth (e.g., Bilek and Lay, 2018; Walton et al., 2021; Wirth et al., 2022). Physics-based numerical models help to investigate the underlying processes that govern their occurrence and impact (e.g., Oglesby et al., 1998; Noda and Lapusta, 2013). For example, *Sequences of Earthquakes and Aseismic Slip* (*SEAS*) models can be used to study spontaneous earthquake and slow slip events driven by tectonic loading over many seismic cycles (e.g., Lapusta et al., 2000; Erickson et al., 2020). SEAS models have been used to study the influence of sedimentary basin effects on the earthquake cycle (Erickson and Dunham, 2014), the effects of fault bends on rupture arrest (Ozawa et al., 2023), or the effect of megathrust fault geometry on simulated slip patterns (Biemiller et al., 2024). Earthquake dynamic rupture simulations, on the other hand, can be used to study earthquake dynamics and seismic wave propagation (Ramos et al., 2022), providing valuable insight into complex rupture processes (Andrews, 1976). These simulations are routinely applied to dipping fault geometries in 3D media (e.g., Mikumo and Miyatake, 1993), and many recent studies focus on effects caused by different assumptions on friction parameters, prestress, and subsurface structure (Kaneko et al., 2008; Tinti et al., 2021; Liu and Becker, 2025; Glehman et al., 2025).

Numerical simulations are also critical for understanding how seafloor deformation causes tsunami generation (e.g., Satake et al., 2003; Titov et al., 2005; Harig et al., 2008). Different models of earthquake rupture have been used to investigate the effects of splay faulting, shallow slip and near-trench uplift, rupture kinematics, as well as structural variations on tsunami generation (e.g., Wendt et al., 2009; Williamson et al., 2019; Du et al., 2021; Small et al., 2025; Dunham et al., 2025). Other modeling efforts improve tsunami hazard mitigation through vulnerability studies, evaluation of methods for aligning modeled and observed tsunami arrival times, and tsunami hazard assessment (Dengler et al., 2008; Priest et al., 2014; Romano et al., 2020; Dolcimascolo et al., 2022).

Modelers and the community need to be able to trust

*Corresponding author: lbachelo@uoregon.edu

the results of complex numerical simulations. To build trust, modelers can test their codes on predefined scenarios (i.e., benchmarks) and compare their results with each other. Such community code verification exercises have long been the standard in the earthquake dynamic rupture community, led jointly by the *U.S. Geological Survey* (*USGS*) and the *Southern California Earthquake Center*, now *Statewide California Earthquake Center* (*SCEC*; Harris et al. (2009, 2011); Barall and Harris (2014); Harris et al. (2018)). These exercises have more recently been extended to SEAS simulations (Erickson et al., 2020; Jiang et al., 2022; Erickson et al., 2023; Lambert et al., 2025) and, independently of the SCEC efforts, volcano deformation (Crozier et al., 2023). Several other verification and validation benchmarks have been developed for tsunami and inundation modeling involving various sources and environments (Synolakis et al., 2008; Nicolsky et al., 2011; Park et al., 2013; Horrillo et al., 2015; Romano et al., 2016). Here, we distinguish code verification from code validation. Our focus lies on code verification using benchmark problem setups for which no analytical solutions exist. This approach involves different numerical software solving the same equations for the same model geometry, boundary conditions, initial conditions, and parameters (e.g., van Zelst et al., 2022). In contrast, we consider code validation to be the comparison of simulated data with observed (paleo-)data, including seismic, geodetic, or tsunami recordings (e.g., An et al., 2014; Arcos and LeVeque, 2015; Staisch et al., 2024). This report focuses on benchmark-based code verification.

To address the need for a standardized verification framework, we provide an open-access web interface with an *Amazon Web Services (AWS)* backend (Section 2). This platform aims to facilitate future benchmark comparisons. An online platform also supports *FAIR* (*Findable, Accessible, Interoperable, Reusable*; Wilkinson et al. (2016)) assessment of different modeling results. Examples of online platforms include the SRCMOD database for the comparison of finite-fault rupture models (Mai et al., 2016), and the Coupling Cloud, a community database of megathrust kinematic coupling models (Oryan et al., 2026). Cloud computing is increasingly used in geophysics, allowing computational resources to be scaled on demand to accommodate larger simulations and datasets, while avoiding transfer of large data (Arrowsmith et al., 2022; Folch et al., 2023; Krauss et al., 2023; Ni et al., 2025). Cloud computing can also enhance geophysical training activities, with accessible computing environments through the Jupyter ecosystem (Project Jupyter et al., 2018) and trainings (Denolle et al., 2025). As part of the *Cascadia Region Earthquake Science Center (CRESCENT)* (Melgar et al., 2024), several other community web-based platforms have been established, such as for community fault and velocity models and paleoseismic data (Bahavar et al., 2025a,b,c).

2 Implementation and Architecture

Here, we present a code verification platform built on a modular architecture divided into two parts. A web-based uploader interface, developed using the React JavaScript library, to allow users to upload and manage their files, available at this url: https://det-uploader.cascadiaquakes.org (login required, Fig. 3). A data visualization dashboard built with Plotly Dash provides interactive, browser-based plots for exploring and analyzing results available at this url: https://det.cascadiaquakes.org (no login required, Fig. 4). The backend relies on several AWS services (Amazon Web Services, 2026) (Figs. 1 & 2):

- **S3 (Simple Storage Service)** is used to store all uploaded files. S3 is a cloud-based object storage service capable of holding virtually unlimited data in any format, with pricing that scales according to storage volume and data access. This makes it ideal for the potentially large simulation files used in code verification.
- **ECS (Elastic Container Service)** runs the viewer application inside Docker containers. Containers package code and software dependencies together so the application behaves consistently everywhere. ECS automatically manages and scales these containers depending on demand, ensuring the viewer is always responsive.
- **ECR (Elastic Container Registry)** is a versioned library of all containerized applications, built to seamlessly integrate with ECS.
- **AWS Lambda functions** are short (15 minutes max, usually under 5 minutes), on-demand computations. They do not require a constantly running server and are perfect for event-driven tasks. They help reduce costs while remaining extremely scalable, since you can run many Lambdas in parallel during periods of high demand. In our workflow, we use it to process the uploaded data.
- **Step Functions** coordinate the processing workflow by managing all the events and starting the next computation following a logic tree. This is used to better handle errors, retries, and logging of the pre-processing.
- **Cognito** is AWS authentication service. It manages login, security, and permissions so users can safely manage their files.
- **CloudFront** is a global content-delivery network that delivers the front-end website to users.

These different services help support the modularity, scalability, and maintainability of the entire project.

To ensure consistency and flexibility across the platform, each benchmark is described by a JSON file that defines its structure. This includes the types of outputs (e.g., time series or surface grids), variable names and units, file types, and any associated metadata. The uploader uses this descriptor to validate inputs and route them correctly, while the viewer uses it to organize outputs and label them appropriately. By externalizing the benchmark definition, the system becomes fully modular: new benchmarks can be added by introducing a new JSON file, with no changes required to the underlying logic of the uploader or viewer. Listing 1 shows an example of the JSON benchmark description.

Listing 1 Example benchmark descriptor JSON file showing a time-series and a surface output entry. Describing the benchmark's expected data and format allows both preprocessing and visualization to be fully parametric. Adding a new benchmark requires only a new JSON descriptor.

```
{
  "name": "ttpv1",
  "files": [
    {
      "name": "fault",
      "content": "receivers on-fault",
      "graph_type": "timeseries",
      "list_of_receivers": [
        "faultst000dp000",
        "faultst000dp010"
      ],
      "var_list": [
        { "name": "t",      "unit": "s", "
            description": "time" },
        { "name": "h-slip", "unit": "m", "
            description": "horizontal slip"
            },
        { "name": "v-slip", "unit": "m", "
            description": "vertical slip" }
      ],
      "file_type": "csv"
    },
    {
      "name": "Seafloor",
      "content": "surface deformation at end
          of simulation",
      "graph_type": "surface",
      "list_of_receivers": [
        "surfdef"
      ],
      "grid": {
        "x": { "min": -100000.0, "max":
            100000.0, "n": 1001 },
        "y": { "min": -100000.0, "max":
            100000.0, "n": 1001 }
      },
      "var_list": [
        { "name": "x",      "unit": "m", "
            description": "distance along x"
            },
        { "name": "y",      "unit": "m", "
            description": "distance along y"
            },
        { "name": "z-disp", "unit": "m", "
            description": "vertical
            displacement" }
      ],
      "file_type": "csv"
    }
  ]
}
```

2.1 The uploader

We designed the uploader (https://det-uploader.cascadiaquakes.org) to provide a secure, cloud-based system for collecting and managing model output files submitted by the community, formatted according to the benchmark specification. The infrastructure is built entirely on AWS and leverages a serverless architecture for scalability and minimal maintenance. A schematic of the full architecture is shown in Fig. 1.

The frontend is a single-page React application hosted on Amazon S3 and served via CloudFront. User authentication is handled with AWS Cognito. After logging in, users can upload their results as a .zip file directly to S3. For example, for both "The Tsunami Problem Versions", that is TTPV1 & TTPV2, this includes receiver time-series ASCII files adhering to naming conventions and file size requirements for 2D surface output files (Kutschera et al., 2025). Uploads are restricted by AWS Identity and Access Management (IAM) policies tied to each user session.

Each new upload triggers an AWS Step Functions state machine that manages backend processing:

1. A Lambda function retrieves the uploaded ZIP from S3. The Lambda function loads a benchmark-specific JSON template from S3. This template is used first to identify expected output files by prefix and extension.

2. Tabular structure of these files is parsed and validated against the required variable list.

3. Benchmark defined interpolation/regridding is applied onto a prescribed grid using k-nearest-neighbor inverse-distance weighting. This approach was developed in collaboration with the modelers participating in the TTPV1 & 2 benchmarks to create the most numerically accurate comparison on the platform, especially for cross-sections. But to ensure data integrity, the original files are kept for detailed analysis offline.

4. Processed outputs are stored as Parquet and written to a standardized S3 path by benchmark, code name, and version, along with a generated metadata JSON file containing extracted header information and a list of processed files.

Processing status and errors are recorded in DynamoDB to support user-facing progress reporting. Both validation of the file format and preprocessing are dictated by the JSON benchmark description file (Listing 1).

Processing results and logs are stored in a DynamoDB table, which the frontend polls periodically to report status to the user. This approach provides feedback without requiring persistent connections. The system also supports archiving outputs or integrating them into other downstream tools.

We use AWS Cloud Development Kit (CDK) to define the cloud infrastructure using real programming languages, here Python, which allows for reproducible deployment and version control of the uploader system, excluding the React app. The modular design enables us to easily extend the pipeline for additional file types or validation rules.

2.2 Viewer

The visualization interface is a Dash web application built using Plotly and deployed as a Docker container on

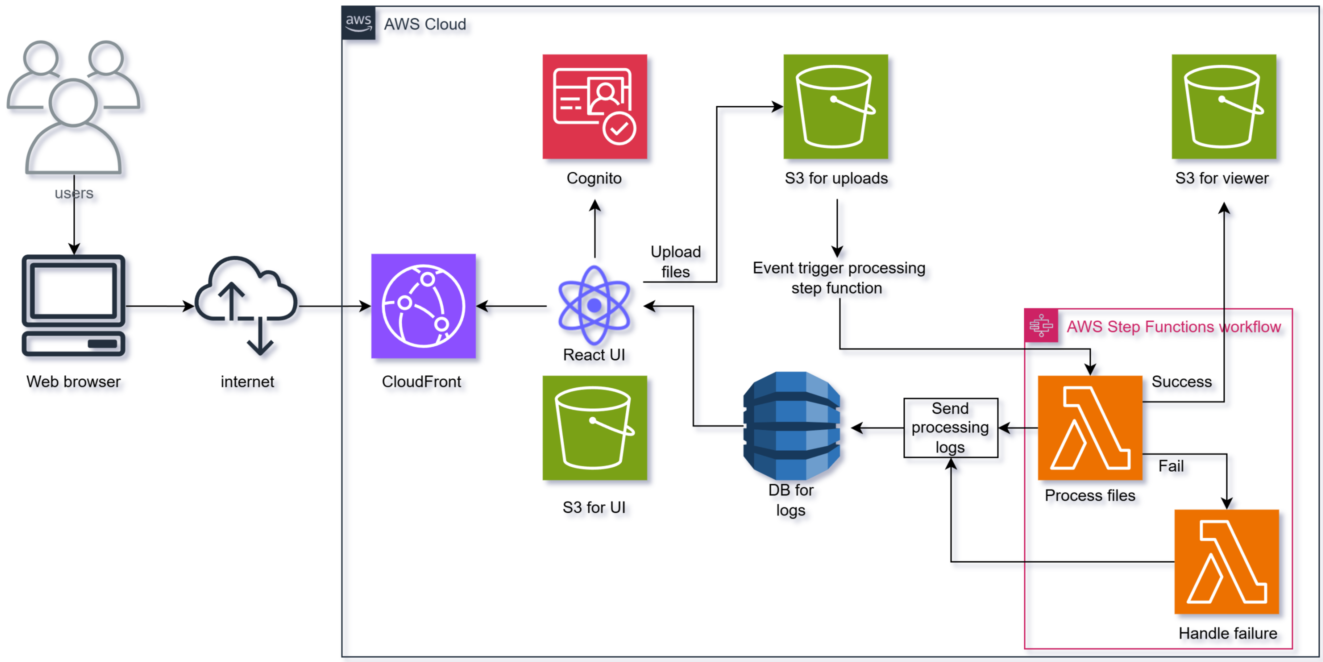

Figure 1 Diagram of the simulation results upload and processing workflow. The users upload the results (all files required as part of the benchmark) as a .zip through a React frontend accessible after login with AWS Cognito. The .zip is uploaded to a temporary S3 bucket, triggering the Step Function. The first step is a Lambda processing the files. Logs are sent to a dynamo DB and read in the frontend, giving feedback to the users. as the files are being processed, they are uploaded to another S3 for the dashboard to access. If there is an issue during the processing, the step function triggers another lambda to handle the failure.

AWS Fargate. It is designed to be fully modular and automatically adapts to the structure of each benchmark based on the corresponding JSON descriptor.

When a user accesses the viewer, the application reads benchmark outputs stored in S3 in Parquet format. The descriptor file defines the list of available outputs, variable names and units, and the graph type to use for each. Based on this information, the viewer dynamically renders time series plots, surface grids, or other appropriate visualizations. This design allows the same frontend to support a wide range of benchmark types without modifying the underlying code.

The Dash app is packaged as a container and stored in ECR. It is launched as a Fargate task behind a load balancer, which routes user traffic. A schematic of the deployment is shown in Fig. 2. This architecture ensures scalability and simplifies updates, as new versions of the viewer can be deployed by pushing a new container image.

The application supports interactive selection of receivers and variables, and automatically updates plots based on user input. Output files are read directly from S3 and only the relevant data is loaded into memory, allowing the viewer to handle large benchmark datasets efficiently. No login is required to access the viewer, enabling open, transparent access to benchmark results and facilitating broad international participation. Users can sign up for secure access to the file management in the uploader (Fig. 3). Additionally, users can upload a single local file for quick comparison without authentication. These temporary uploads are not stored, but allow users to preview and explore their own results using the same visualization interface (Figs. 4 & 5).

2.3 Current benchmarks and supported simulation output

This platform was initially developed for the CRESCENT/SCEC/USGS benchmark exercises “The Tsunami Problem Versions” TTPV1 and TTPV2 (Kutschera et al., 2025). These benchmarks consider spontaneous 3D earthquake dynamic rupture on a 15-degree-dipping thrust fault and tsunami generation using fully coupled solid Earth-ocean governing equations (e.g., Maeda and Furumura, 2013; Lotto and Dunham, 2015; Wilson and Ma, 2021; Krenz et al., 2021; Abrahams et al., 2023). Both problems use the same material parameters and follow the same dynamic rupture model setup, but differ in terms of the added water layer thickness. While TTPV1 has a 1 km thick uniform water layer atop the solid Earth, TTPV2 has a water layer with variable depth, with 3 km water depth on the seaward side, sloping to shallow depth (∼50 m) landwards. The outputs of these benchmarks are time series at selected receivers (same locations across all the simulations Fig. 5), recording time-series data such as displacement, velocity, and pressure. Other recorded outputs include surface data for selected time steps, such as seafloor deformation or sea surface height (Fig. 4). Because each modeling software produces outputs on its own mesh, the spatial locations of variables do not initially match. For consistent visualization and cross-section extraction, we interpolate all results onto a standardized grid shared by all

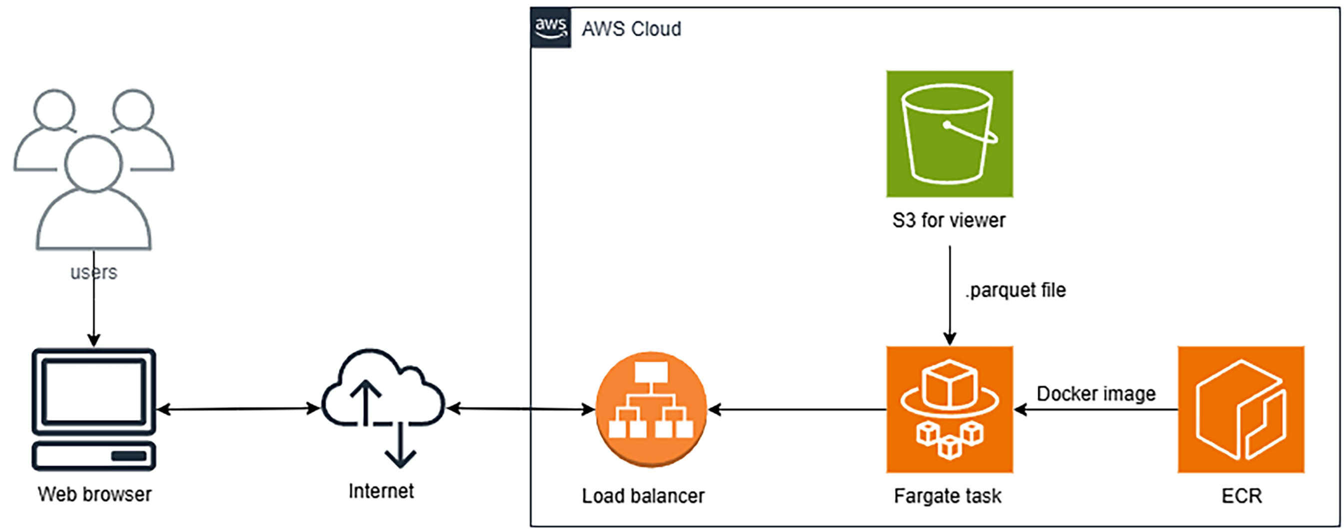

Figure 2 Diagram of the viewer architecture. The viewer is a simple architecture leveraging AWS ECS to run the Dash dashboard container serving it behind an application load balancer. The data are read directly from S3 as parquet files, and the dashboard plots, titles, and units are set using the benchmark JSON description.

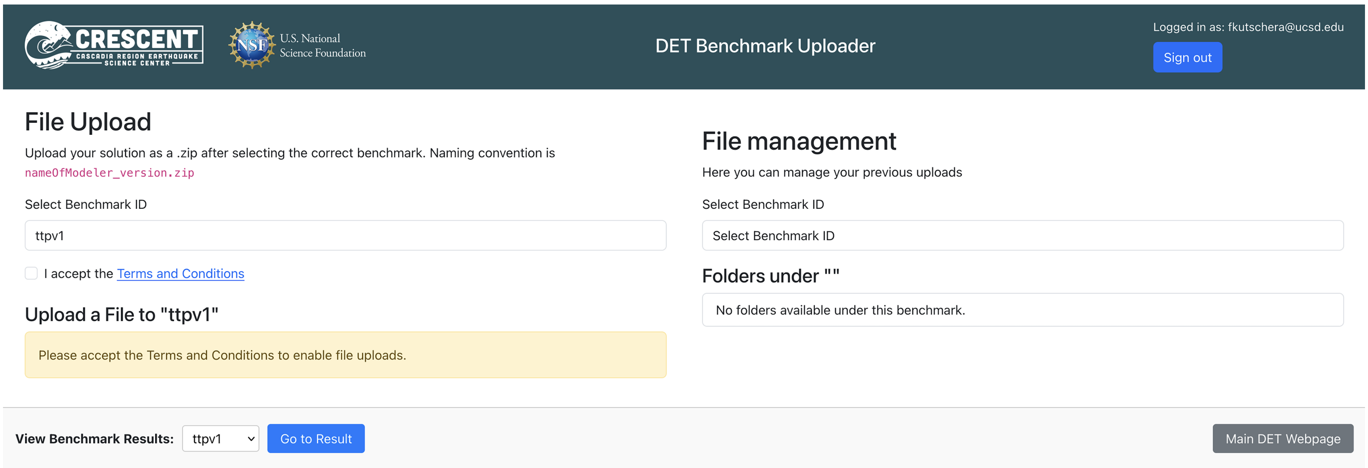

Figure 3 Screenshot of the uploader to the *DET (Dynamic Rupture, Earthquake Cycle, and Tsunamis Working Group)* Code Verification Platform. We welcome new users who simply need to request access by filling out a short form on the website (https://det-uploader.cascadiaquakes.org). Users with accounts may manage their uploads after accepting the terms and conditions.

models (Section 2.1).

3 Future work and takeaways

The platform is designed to remain a long-term, extensible resource for the community, with continued hosting of new CRESCENT and partner benchmarks as they are developed. All benchmarks and their associated results are publicly accessible through the online viewer, enabling researchers to verify their codes against existing solutions without needing access to the underlying raw data. This design preserves modelers' ownership of their original datasets and allows them to retain control over how their data are shared and distributed. This provides a sustainable pathway for ongoing verification as codes evolve. Future enhancements could include the implementation of quantitative comparison metrics among the simulation results (e.g., Barall and Harris, 2014), as well as the addition of new capabilities required for other benchmark types, such as earthquake cycle simulations (e.g., Erickson et al., 2020; Lambert et al., 2025).

In developing this platform (accessible through https://cascadiaquakes.org/det), we emphasized improving upon the existing SCEC dynamic earthquake rupture code comparison platform (https://strike.scec.org/cvws; e.g., Harris et al. (2018)). We have started this project by hosting two benchmarks for 3D dynamic earthquake rupture and tsunami generation, making the platform capable of plotting and comparing sensors, time series, and surface data. The system architecture is benchmark-agnostic and configurable, enabling additional benchmark definitions to be incorporated without modification to the core infrastructure.

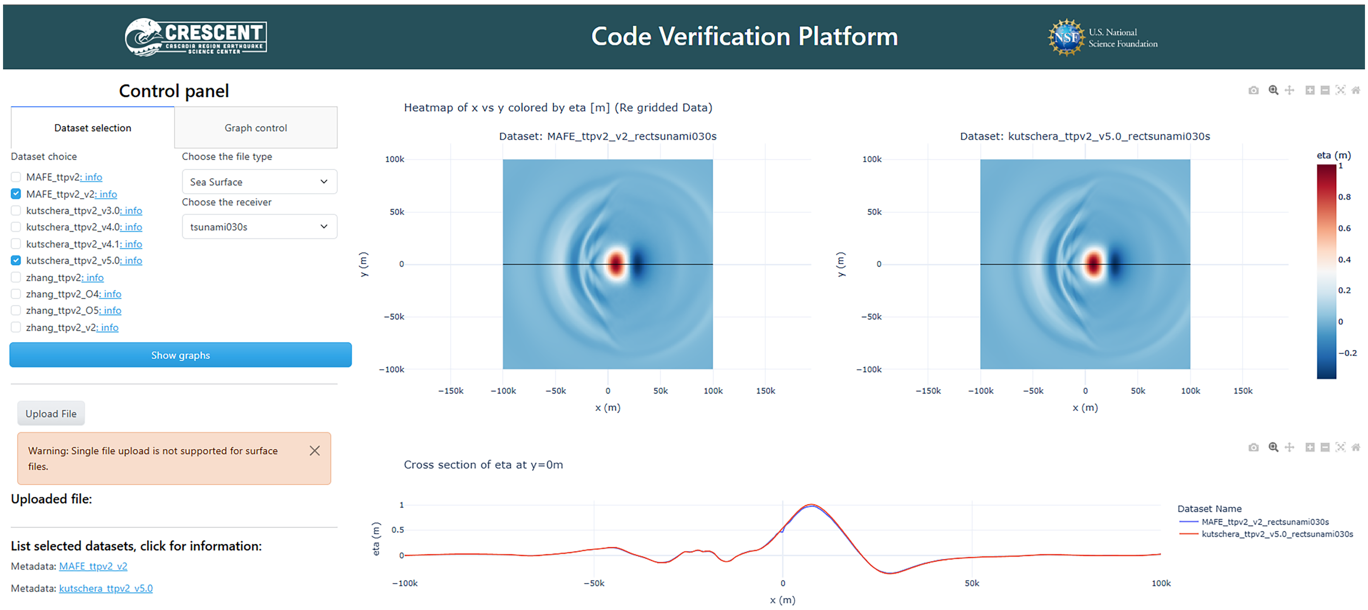

Figure 4 Screenshot of the platform: Left panel is the controls, including the dataset selection, and simple graph controls such as the colorbar range, but also the possibility to change the cross-section along the y-axis. On the right is the interactive visualization, showing an example of the vertical displacement of the sea surface (eta) as well as the corresponding cross-section shown in the upper figures as the horizontal line at $Y = 0$. This example visualizes the simulated sea surface data for *"The Tsunami Problem Version 2" (TTPV2)* after 30 s using the numerical codes MAFE (Ma and Nie, 2019) and SeisSol (Gabriel et al., 2025).

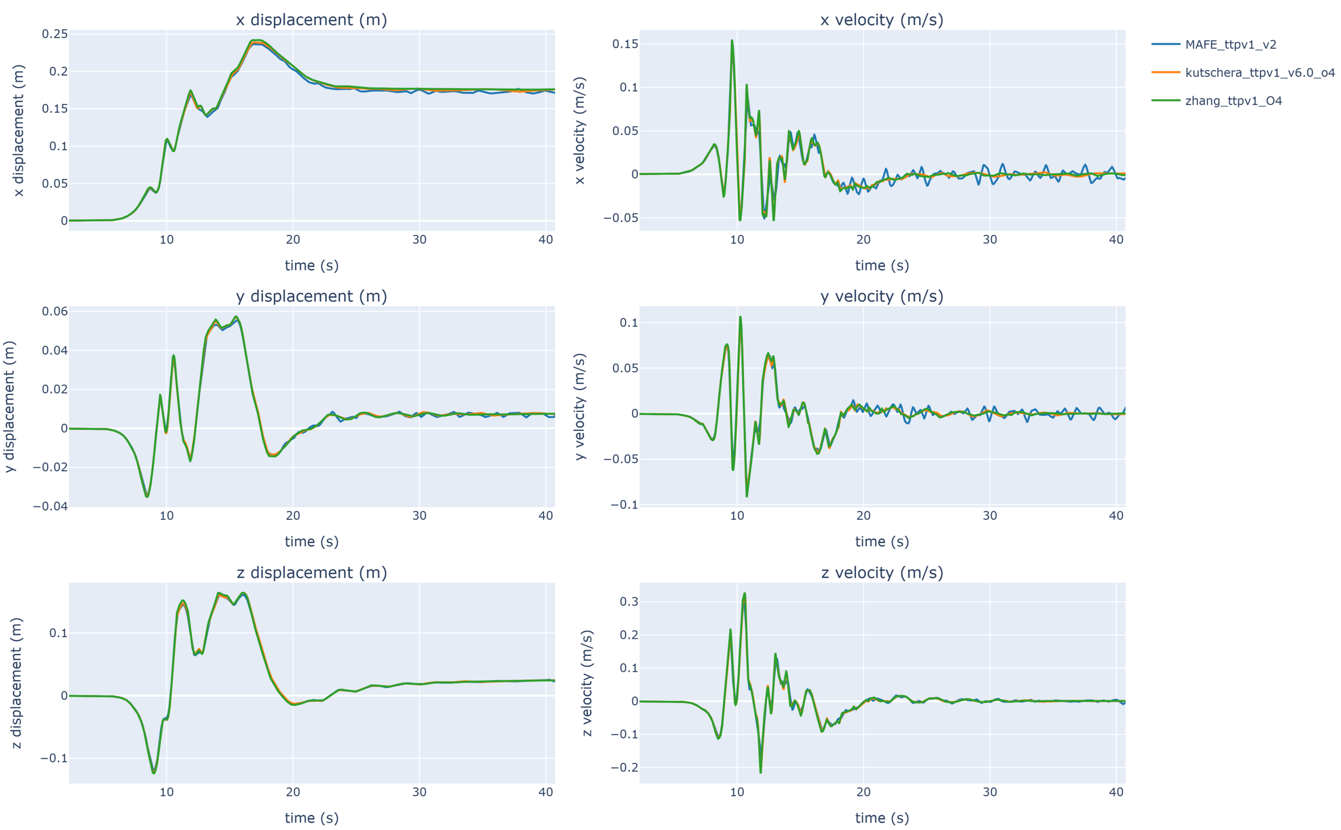

Figure 5 Visualization of an exemplary receiver (el_sf_body030st100; see Kutschera et al., 2025) at the seafloor (solid Earth), showing the unfiltered three-components of velocities and displacements for *"The Tsunami Problem Version 1" (TTPV1)* using the three numerical codes MAFE (Ma and Nie, 2019), SeisSol (Gabriel et al., 2025), and drdg3d (Zhang et al., 2023). Note the different y-axis ranges for each panel.

Acknowledgements

We thank the editor, Marlon Ramos, as well as the reviewers, Tim Clements and an anonymous reviewer, for their insightful comments, which helped us improve the quality of the manuscript. We also thank the broader CRESCENT DET community for their feedback on the platform and CRESCENT developer William Marfo for his contributions to the platform's CI/CD infrastructure and backend tooling. This research was supported by the Cascadia Region Earthquake Science Center (CRESCENT). CRESCENT is funded by the National Science Foundation Cooperative Agreement #2225286. Additional funding is provided by the United States Geological Survey Cooperative Agreement #G25AC00531 and by Pacific Gas and Electric (PG&E). FK and AAG acknowledge additional support from the National Science Foundation (Quakeworx, grant No. OAC-2311208) and gratefully acknowledge the Gauss Centre for Supercomputing e.V. (www.gauss-centre.eu, project pn49ha) for funding this project by providing computing time on the GCS Supercomputer SuperMUC-NG at Leibniz Supercomputing Centre (www.lrz.de). AAG acknowledges additional support from the National Science Foundation (grants EAR-2121568, OAC-2139536, RISE-2531036), Horizon Europe (grants No. 101093038, 101058129, 101058518), USGS NEHRP award No. G26AP00141 and NASA (grant No. 80NSSC20K0495).

Any use of trade, firm, or product names is for descriptive purposes only and does not imply endorsement by the U.S. Government.

Data and code availability

All source code developed for this study is open source and publicly available. The web-based visualization dashboard is maintained at https://github.com/cascadiaquakes/v-v_dashboard, and the secure file management and upload system is maintained at https://github.com/cascadiaquakes/det-file-manager.

These repositories contain the full implementation of the user interfaces, application logic, and supporting infrastructure configuration required to reproduce the software described in this report. As GitHub is not a persistent archival repository, a citable snapshot of each repository has been archived on Zenodo and assigned a DOI: Uploader https://doi.org/10.5281/zenodo.20673090, visualization dashboard https://doi.org/10.5281/zenodo.20673098.

All links specified in this software report were last accessed on 14 July 2026.

Competing interests

The authors have no competing interests.

References

Abrahams, L. S., Krenz, L., Dunham, E. M., Gabriel, A.-A., and Saito, T. Comparison of Methods for Coupled Earthquake and Tsunami Modelling. *Geophysical Journal International*, 234(1):404–426, 2023. doi: 10.1093/gji/ggad053.

Amazon Web Services. Overview of Amazon Web Services. Technical report, Amazon Web Services, Inc., 2026. https://docs.aws.amazon.com/whitepapers/latest/aws-overview/aws-overview.pdf. AWS Whitepaper, accessed February 2026.

An, C., Sepúlveda, I., and Liu, P. L.-F. Tsunami Source and Its Validation of the 2014 Iquique, Chile, Earthquake. *Geophysical Research Letters*, 41(11):3988–3994, 2014. doi: 10.1002/2014GL060567.

Andrews, D. J. Rupture Velocity of Plane Strain Shear Cracks. *Journal of Geophysical Research*, 81(32):5679–5687, 1976. doi: 10.1029/JB081I032P05679.

Arcos, M. E. and LeVeque, R. J. Validating Velocities in the GeoClaw Tsunami Model Using Observations near Hawaii from the 2011 Tohoku Tsunami. *Pure and Applied Geophysics*, 172(3-4): 849–867, 2015. doi: 10.1007/s00024-014-0980-y.

Arrowsmith, S. J., Trugman, D. T., MacCarthy, J., Bergen, K. J., Lumley, D., and Magnani, M. B. Big Data Seismology. *Reviews of Geophysics*, 60(2):e2021RG000769, 2022. doi: 10.1029/2021RG000769.

Bahavar, M., Delph, J., Ashraf, A., Share, P.-E., Sahakian, V., Thomas, A., Bachelot, L., Hooft, E., Ajala, R., and Group, C. C. W. The Cascadia Region Earthquake Science Center (CRESCENT) Community Velocity Model Viewer. Zenodo, 2025a. doi: 10.5281/zenodo.15015094.

Bahavar, M., Staisch, L., Dura, T., Hawkes, A., Kelsey, H., La Selle, S., Witter, R., Bruce, D., Bachelot, L., and Thomas, A. The Cascadia Region Earthquake Science Center (CRESCENT) Paleoseismic Viewer. Zenodo, 2025b. doi: 10.5281/zenodo.15866114.

Bahavar, M., Styron, R., Streig, A., Thomas, A., Bachelot, L., and CRESCENT CFM working group. The Cascadia Region Earthquake Science Center (CRESCENT) Community Fault Model Viewer. Zenodo, 2025c. doi: 10.5281/zenodo.15021860.

Barall, M. and Harris, R. A. Metrics for Comparing Dynamic Earthquake Rupture Simulations. *Seismological Research Letters*, 86 (1):223–235, 2014. doi: 10.1785/0220140122.

Biemiller, J., Gabriel, A.-A., May, D. A., and Staisch, L. Subduction Zone Geometry Modulates the Megathrust Earthquake Cycle: Magnitude, Recurrence, and Variability. *Journal of Geophysical Research: Solid Earth*, 129(8):e2024JB029191, 2024. doi: 10.1029/2024JB029191.

Bilek, S. L. and Lay, T. Subduction Zone Megathrust Earthquakes. *Geosphere*, 14(4):1468–1500, 2018. doi: 10.1130/GES01608.1.

Crozier, J., Karlstrom, L., Montgomery-Brown, E., Angarita, M., Cayol, V., Bato, M. G., Wang, T. A., Grapenthin, R., Shreve, T., Anderson, K., Astort, A., Bodart, O., Cannavò, F., Currenti, G., Dabaghi, F., Erickson, B. A., Garg, D., Head, M., Iozzia, A., Kim, Y. C., Le Mével, H., Novoa Lizama, C., Rucker, C., Silverii, F., Trasatti, E., and Zhan, Y. Understanding the Drivers of Volcano Deformation through Geodetic Model Verification and Validation. *Bulletin of Volcanology*, 85(12):74, 2023. doi: 10.1007/s00445-023-01687-4.

Dengler, L., Uslu, B., Barberopoulou, A., Borrero, J., and Synolakis, C. The Vulnerability of Crescent City, California, to Tsunamis Generated by Earthquakes in the Kuril Islands Region of the Northwestern Pacific. *Seismological Research Letters*, 79(5): 608–619, 2008. doi: 10.1785/gssrl.79.5.608.

Denolle, M. A., Tape, C., Bozdağ, E., Wang, Y., Waldhauser, F., Gabriel, A.-A., Braunmiller, J., Chow, B., Ding, L., Feng, K.-F., Ghosh, A., Groebner, N., Gupta, A., Krauss, Z., McPherson, A. M., Nagaso, M., Niu, Z., Ni, Y., Örsvuran, R., Pavlis, G., Rodriguez-Cardozo, F., Sawi, T., Schaff, D., Schliwa, N., Schneller, D., Shi, Q., Thurin, J., Wang, C., Wang, K., Wong, J. W. C., Wolf, S., and Yuan, C. Training the Next Generation of

Seismologists: Delivering Research-Grade Software Education for Cloud and HPC Computing Through Diverse Training Modalities. *Seismological Research Letters*, 96(5):3265–3279, 2025. doi: 10.1785/0220240413.

Dolcimascolo, A., Eungard, D. W., Allen, C., LeVeque, R. J., Adams, L., Arcas, D., Titov, V. V., González, F. I., Moore, C., and Garrison-Laney, C. E. Tsunami Hazard Maps of the Puget Sound and Adjacent Waters – Model Results from a 2,500-Year Magnitude 9.0 Cascadia Subduction Zone Earthquake Scenario: Washington Geological Survey Map Series 2021-01, 16 Sheets, Scale 1:48,000. *Washington Geological Survey*, 2022.

Du, Y., Ma, S., Kubota, T., and Saito, T. Impulsive Tsunami and Large Runup Along the Sanriku Coast of Japan Produced by an Inelastic Wedge Deformation Model. *Journal of Geophysical Research: Solid Earth*, 126(8):e2021JB022098, 2021. doi: 10.1029/2021JB022098.

Dunham, A. M., Kim, J., Wirth, E., Schmidt, D., LeVeque, R. J., Wei, Y., Adams, L. M., and Pollitz, F. The Impact of 3D Structure on Coseismic Coastal Land-Level Change and Tsunami Generation in the Cascadia Subduction Zone. *Geophysical Research Letters*, 52(24):e2025GL117783, 2025. doi: 10.1029/2025GL117783.

Erickson, B. A. and Dunham, E. M. An Efficient Numerical Method for Earthquake Cycles in Heterogeneous Media: Alternating Subbasin and Surface-Rupturing Events on Faults Crossing a Sedimentary Basin. *Journal of Geophysical Research: Solid Earth*, 119(4):3290–3316, 2014. doi: 10.1002/2013JB010614.

Erickson, B. A., Jiang, J., Barall, M., Lapusta, N., Dunham, E. M., Harris, R., Abrahams, L. S., Allison, K. L., Ampuero, J.-P., Barbot, S., Cattania, C., Elbanna, A., Fialko, Y., Idini, B., Kozdon, J. E., Lambert, V., Liu, Y., Luo, Y., Ma, X., Best McKay, M., Segall, P., Shi, P., van den Ende, M., and Wei, M. The Community Code Verification Exercise for Simulating Sequences of Earthquakes and Aseismic Slip (SEAS). *Seismological Research Letters*, 91(2A):874–890, 2020. doi: 10.1785/0220190248.

Erickson, B. A., Jiang, J., Lambert, V., Barbot, S. D., Abdelmeguid, M., Almquist, M., Ampuero, J.-P., Ando, R., Cattania, C., Chen, A., Dal Zilio, L., Deng, S., Dunham, E. M., Elbanna, A. E., Gabriel, A.-A., Harvey, T. W., Huang, Y., Kaneko, Y., Kozdon, J. E., Lapusta, N., Li, D., Li, M., Liang, C., Liu, Y., Ozawa, S., Perez-Silva, A., Pranger, C., Segall, P., Sun, Y., Thakur, P., Uphoff, C., van Dinther, Y., and Yang, Y. Incorporating Full Elastodynamic Effects and Dipping Fault Geometries in Community Code Verification Exercises for Simulations of Earthquake Sequences and Aseismic Slip (SEAS). *Bulletin of the Seismological Society of America*, 113(2):499–523, 2023. doi: 10.1785/0120220066.

Folch, A., Abril, C., Afanasiev, M., Amati, G., Bader, M., Badia, R. M., Bayraktar, H. B., Barsotti, S., Basili, R., Bernardi, F., Boehm, C., Brizuela, B., Brogi, F., Cabrera, E., Casarotti, E., Castro, M. J., Cerminara, M., Cirella, A., Cheptsov, A., Conejero, J., Costa, A., de la Asunción, M., de la Puente, J., Djuric, M., Dorozhinskii, R., Espinosa, G., Esposti-Ongaro, T., Farnós, J., Favretto-Cristini, N., Fichtner, A., Fournier, A., Gabriel, A.-A., Gallard, J.-M., Gibbons, S. J., Glimsdal, S., González-Vida, J. M., Gracia, J., Gregorio, R., Gutierrez, N., Halldorsson, B., Hamitou, O., Houzeaux, G., Jaure, S., Kessar, M., Krenz, L., Krischer, L., Laforet, S., Lanucara, P., Li, B., Lorenzino, M. C., Lorito, S., Løvholt, F., Macedonio, G., Macías, J., Marín, G., Martínez Montesinos, B., Mingari, L., Moguilny, G., Montellier, V., Monterrubio-Velasco, M., Moulard, G. E., Nagaso, M., Nazaria, M., Niethammer, C., Pardini, F., Pienkowska, M., Pizzimenti, L., Poiata, N., Rannabauer, L., Rojas, O., Rodriguez, J. E., Romano, F., Rudyy, O., Ruggiero, V., Samfass, P., Sánchez-Linares, C., Sanchez, S., Sandri, L., Scala, A., Schaeffer, N., Schuchart, J., Selva, J., Sergeant, A., Stallone, A., Taroni, M., Thrastarson, S., Titos, M., Tonelllo, N., Tonini, R., Ulrich, T., Vilotte, J.-P., Vöge, M., Volpe, M., Aniko Wirp, S., and Wössner, U. The EU Center of Excellence for Exascale in Solid Earth (ChEESE): Implementation, Results, and Roadmap for the Second Phase. *Future Generation Computer Systems*, 2023. doi: 10.1016/J.FUTURE.2023.04.006.

Gabriel, A.-A., Kurapati, V., Niu, Z., Schliwa, N., Schneller, D., Ulrich, T., Dorozhinskii, R., Krenz, L., Uphoff, C., Wolf, S., Breuer, A., Heinecke, A., Pelties, C., Rettenberger, S., Wollherr, S., and Bader, M. SeisSol. Zenodo, 2025. doi: 10.5281/zenodo.4672483.

Glehman, J., Gabriel, A., Ulrich, T., Ramos, M., Huang, Y., and Lindsey, E. Partial Ruptures Governed by the Complex Interplay between Geodetic Slip Deficit, Rigidity, and Pore Fluid Pressure in 3D Cascadia Dynamic Rupture Simulations. *Seismica*, 2(4), 2025. doi: 10.26443/seismica.v2i4.1427.

Harig, S., Chaeroni, Pranowo, W. S., and Behrens, J. Tsunami Simulations on Several Scales. *Ocean Dynamics*, 58(5):429–440, 2008. doi: 10.1007/s10236-008-0162-5.

Harris, R. A., Barall, M., Archuleta, R., Dunham, E., Aagaard, B., Ampuero, J. P., Bhat, H., Cruz-Atienza, V., Dalguer, L., Dawson, P., Day, S., Duan, B., Ely, G., Kaneko, Y., Kase, Y., Lapusta, N., Liu, Y., Ma, S., Oglesby, D., Olsen, K., Pitarka, A., Song, S., and Templeton, E. The SCEC/USGS Dynamic Earthquake Rupture Code Verification Exercise. *Seismological Research Letters*, 80(1):119–126, 2009. doi: 10.1785/gssrl.80.1.119.

Harris, R. A., Barall, M., Andrews, D. J., Duan, B., Ma, S., Dunham, E. M., Gabriel, A.-A., Kaneko, Y., Kase, Y., Aagaard, B. T., Oglesby, D. D., Ampuero, J.-P., Hanks, T. C., and Abrahamson, N. Verifying a Computational Method for Predicting Extreme Ground Motion. *Seismological Research Letters*, 82(5):638–644, 2011. doi: 10.1785/gssrl.82.5.638.

Harris, R. A., Aagaard, B., Barall, M., Ma, S., Roten, D., Olsen, K., Duan, B., Liu, D., Luo, B., Bai, K., Ampuero, J. P., Kaneko, Y., Gabriel, A. A., Duru, K., Ulrich, T., Wollherr, S., Shi, Z., Dunham, E., Bydlon, S., Zhang, Z., Chen, X., Somala, S. N., Pelties, C., Tago, J., Cruz-Atienza, V. M., Kozdon, J., Daub, E., Aslam, K., Kase, Y., Withers, K., and Dalguer, L. A Suite of Exercises for Verifying Dynamic Earthquake Rupture Codes. *Seismological Research Letters*, 89(3):1146–1162, 2018. doi: 10.1785/0220170222.

Horrillo, J., Grilli, S. T., Nicolsky, D., Roeber, V., and Zhang, J. Performance Benchmarking Tsunami Models for NTHMP's Inundation Mapping Activities. *Pure and Applied Geophysics*, 172(3): 869–884, 2015. doi: 10.1007/s00024-014-0891-y.

Jiang, J., Erickson, B. A., Lambert, V. R., Ampuero, J.-P., Ando, R., Barbot, S. D., Cattania, C., Zilio, L. D., Duan, B., Dunham, E. M., Gabriel, A.-A., Lapusta, N., Li, D., Li, M., Liu, D., Liu, Y., Ozawa, S., Pranger, C., and van Dinther, Y. Community-Driven Code Comparisons for Three-Dimensional Dynamic Modeling of Sequences of Earthquakes and Aseismic Slip. *Journal of Geophysical Research: Solid Earth*, 127(3):e2021JB023519, 2022. doi: 10.1029/2021JB023519.

Kaneko, Y., Lapusta, N., and Ampuero, J.-P. Spectral Element Modeling of Spontaneous Earthquake Rupture on Rate and State Faults: Effect of Velocity-Strengthening Friction at Shallow Depths. *Journal of Geophysical Research: Solid Earth*, 113 (B9), 2008. doi: 10.1029/2007JB005553.

Krauss, Z., Ni, Y., Henderson, S., and Denolle, M. Seismology in the Cloud: Guidance for the Individual Researcher. *Seismica*, 2(2), 2023. doi: 10.26443/seismica.v2i2.979.

Krenz, L., Uphoff, C., Ulrich, T., Gabriel, A. A., Abrahams, L. S., Dunham, E. M., and Bader, M. 3D Acoustic-Elastic Coupling with Gravity: The Dynamics of the 2018 Palu, Sulawesi Earthquake and Tsunami. *International Conference for High Performance Computing, Networking, Storage and Analysis, SC*, 2021. doi: 10.1145/3458817.3476173.

Kutschera, F., Gabriel, A.-A., and Dunham, E. M. CRESCENT

Tsunami Benchmark (TTPV1 and TTPV2): 3D Fully Coupled Earthquake Dynamic Rupture and Tsunami Benchmarks with Varying Bathymetric Complexity. *Zenodo*, 2025. doi: 10.5281/zenodo.15389414.

Lambert, V. R., Erickson, B. A., Jiang, J., Dunham, E. M., Kim, T., Ampuero, J.-P., Ando, R., Cappa, F., Dublanchet, P., Elbanna, A., Fialko, Y., Gabriel, A.-A., Lapusta, N., Li, M., Marcum, J., May, D., Mia, M. S., Ozawa, S., Pranger, C., Romanet, P., Scuderi, M. M., van Dinther, Y., Yang, Y., and Yun, J. Community-Driven Code Comparisons for Simulations of Fluid-Induced Aseismic Slip. *Journal of Geophysical Research: Solid Earth*, 130(4): e2024JB030601, 2025. doi: 10.1029/2024JB030601.

Lapusta, N., Rice, J. R., Ben-Zion, Y., and Zheng, G. Elastodynamic Analysis for Slow Tectonic Loading with Spontaneous Rupture Episodes on Faults with Rate- and State-Dependent Friction. *Journal of Geophysical Research: Solid Earth*, 105(B10): 23765–23789, 2000. doi: 10.1029/2000JB900250.

Liu, D. and Becker, T. W. Earthquake Rupture Dynamics From Graph Neural Networks. *Journal of Geophysical Research: Solid Earth*, 130(12):e2025JB031981, 2025. doi: 10.1029/2025JB031981.

Lotto, G. C. and Dunham, E. M. High-Order Finite Difference Modeling of Tsunami Generation in a Compressible Ocean from Offshore Earthquakes. *Computational Geosciences*, 19(2):327–340, 2015. doi: 10.1007/S10596-015-9472-0.

Ma, S. and Nie, S. Dynamic Wedge Failure and Along-Arc Variations of Tsunamigenesis in the Japan Trench Margin. *Geophysical Research Letters*, 46(15):8782–8790, 2019. doi: 10.1029/2019GL083148.

Maeda, T. and Furumura, T. FDM Simulation of Seismic Waves, Ocean Acoustic Waves, and Tsunamis Based on Tsunami-Coupled Equations of Motion. *Pure and Applied Geophysics*, 170 (1):109–127, 2013. doi: 10.1007/s00024-011-0430-z.

Mai, P. M., Schorlemmer, D., Page, M., Ampuero, J.-P., Asano, K., Causse, M., Custodio, S., Fan, W., Festa, G., Galis, M., Gallovic, F., Imperatori, W., Käser, M., Malytskyy, D., Okuwaki, R., Pollitz, F., Passone, L., Razafindrakoto, H. N. T., Sekiguchi, H., Song, S. G., Somala, S. N., Thingbaijam, K. K. S., Twardzik, C., van Driel, M., Vyas, J. C., Wang, R., Yagi, Y., and Zielke, O. The Earthquake-Source Inversion Validation (SIV) Project. *Seismological Research Letters*, 87(3):690–708, 2016. doi: 10.1785/0220150231.

Melgar, D., Thomas, A. M., Sahakian, V. J., Meigs, A. J., Share, P. E., Tobin, H. J., Melbourne, T. I., and Elizabeth, J. The Cascadia Region Earthquake Science Center Strategic Plan 2023-2027. *CRESCENT Open Documents Library*, 2024. doi: 10.5281/zenodo.11212220.

Mikumo, T. and Miyatake, T. Dynamic Rupture Processes on a Dipping Fault, and Estimates of Stress Drop and Strength Excess from the Results of Waveform Inversion. *Geophysical Journal International*, 112(3):481–496, 1993. doi: 10.1111/j.1365-246X.1993.tb01182.x.

Ni, Y., Denolle, M. A., Münchmeyer, J., Wang, Y., Feng, K.-F., Garcia Jurado Suarez, C., Thomas, A. M., Trabant, C., Hamilton, A., and Mencin, D. A Review of Cloud Computing and Storage in Seismology. *Geophysical Journal International*, 243(1):ggaf322, 2025. doi: 10.1093/gji/ggaf322.

Nicolsky, D. J., Suleimani, E. N., and Hansen, R. A. Validation and Verification of a Numerical Model for Tsunami Propagation and Runup. *Pure and Applied Geophysics*, 168(6):1199–1222, 2011. doi: 10.1007/s00024-010-0231-9.

Noda, H. and Lapusta, N. Stable Creeping Fault Segments Can Become Destructive as a Result of Dynamic Weakening. *Nature*, 493(7433):518–521, 2013. doi: 10.1038/nature11703.

Oglesby, D. D., Archuleta, R. J., and Nielsen, S. B. Earthquakes on Dipping Faults: The Effects of Broken Symmetry. *Science*, 280 (5366):1055–1059, 1998. doi: 10.1126/science.280.5366.1055.

Oryan, B., Gabriel, A.-A., Bürgmann, R. B., Calais, E., Cheng, G., Chlieh, M., Cosenza-Muralles, B., Cruz-Atienza, V. M., Zilio, L. D., DeMets, C., Elliott, J., Ellis, A., Feng, L., Freymueller, J. T., Gunawan, E., Hanifa, N. R., Hilley, G. E., Hsu, Y.-J., Iinuma, T., Itoh, Y., Jara, J., Johnson, K. M., Jolivet, R., Kano, M., Klein, E., Li, S., Li, S., Lindsey, E. O., Liu, Z., Loveless, J. P., Lovery, B., Maubant, L., Michel, S., Muller, C., Métois, M., Nishimura, T., Noda, A., Panda, D., Perry, M., Plata-Martinez, R., Radiguet, M., Rousset, B., Sherrill, E. M., Socquet, A., Villegas-Lanza, J. C., Wallace, L. M., Xue, L., Yokota, Y., Yoshioka, S., and Yu, S.-B. The Coupling Cloud: A Community Database of Megathrust Kinematic Coupling Models. 2026. doi: 10.31223/X5WJ2R.

Ozawa, S., Ando, R., and Dunham, E. M. Quantifying the Probability of Rupture Arrest at Restraining and Releasing Bends Using Earthquake Sequence Simulations. *Earth and Planetary Science Letters*, 617:118276, 2023. doi: 10.1016/j.epsl.2023.118276.

Park, H., Cox, D. T., Lynett, P. J., Wiebe, D. M., and Shin, S. Tsunami Inundation Modeling in Constructed Environments: A Physical and Numerical Comparison of Free-Surface Elevation, Velocity, and Momentum Flux. *Coastal Engineering*, 79:9–21, 2013. doi: 10.1016/j.coastaleng.2013.04.002.

Priest, G. R., Zhang, Y., Witter, R. C., Wang, K., Goldfinger, C., and Stimely, L. Tsunami Impact to Washington and Northern Oregon from Segment Ruptures on the Southern Cascadia Subduction Zone. *Natural Hazards*, 72(2):849–870, 2014. doi: 10.1007/s11069-014-1041-7.

Project Jupyter, Bussonnier, M., Forde, J., Freeman, J., Granger, B., Head, T., Holdgraf, C., Kelley, K., Nalvarte, G., Osheroff, A., Pacer, M., Panda, Y., Perez, F., Ragan-Kelley, B., and Willing, C. Binder 2.0 - Reproducible, Interactive, Sharable Environments for Science at Scale. In *Python in Science Conference*, pages 113–120, 2018. doi: 10.25080/Majora-4af1f417-011.

Ramos, M. D., Thakur, P., Huang, Y., Harris, R. A., and Ryan, K. J. Working with Dynamic Earthquake Rupture Models: A Practical Guide. *Seismological Research Letters*, 93(4):2096–2110, 2022. doi: 10.1785/0220220022.

Romano, A., Di Risio, M., Bellotti, G., Molfetta, M. G., Damiani, L., and De Girolamo, P. Tsunamis Generated by Landslides at the Coast of Conical Islands: Experimental Benchmark Dataset for Mathematical Model Validation. *Landslides*, 13(6):1379–1393, 2016. doi: 10.1007/s10346-016-0696-4.

Romano, F., Lorito, S., Lay, T., Piatanesi, A., Volpe, M., Murphy, S., and Tonini, R. Benchmarking the Optimal Time Alignment of Tsunami Waveforms in Nonlinear Joint Inversions for the Mw 8.8 2010 Maule (Chile) Earthquake. *Frontiers in Earth Science*, 8, 2020.

Satake, K., Wang, K., and Atwater, B. F. Fault Slip and Seismic Moment of the 1700 Cascadia Earthquake Inferred from Japanese Tsunami Descriptions. *Journal of Geophysical Research: Solid Earth*, 108(B11), 2003. doi: 10.1029/2003JB002521.

Small, D. T., Melgar, D., La Selle, S., and Meigs, A. Combining Multi-site Tsunami and Deformation Modeling to Constrain Slip Distributions for the 1700 C.E. Cascadia Earthquake. *Bulletin of the Seismological Society of America*, 115(2):431–451, 2025. doi: 10.1785/0120240218.

Staisch, L., Witter, R., Watt, J., Grant, A., Walton, M., Brothers, D., Davis, E., Dura, C., Engelhart, S., Enkin, R., et al. Compiled Onshore and Offshore Paleoseismic Data along the Cascadia Subduction Zone. 2024. doi: 10.5066/P13OJQYW.

Synolakis, C. E., Bernard, E. N., Titov, V. V., Kânoğlu, U., and González, F. I. Validation and Verification of Tsunami Numerical Models. *Pure and Applied Geophysics*, 165(11):2197–2228, 2008. doi: 10.1007/s00024-004-0427-y.

Tinti, E., Casarotti, E., Ulrich, T., Taufiqurrahman, T., Li, D., and Gabriel, A. A. Constraining Families of Dynamic Models Using Geological, Geodetic and Strong Ground Motion Data: The Mw 6.5, October 30th, 2016, Norcia Earthquake, Italy. *Earth and Planetary Science Letters*, 576:117237, 2021. doi: 10.1016/J.EPSL.2021.117237.

Titov, V., Rabinovich, A. B., Mofjeld, H. O., Thomson, R. E., and González, F. I. The Global Reach of the 26 December 2004 Sumatra Tsunami. *Science*, 309(5743):2045–2048, 2005. doi: 10.1126/science.1114576.

van Zelst, I., Crameri, F., Pusok, A. E., Glerum, A., Dannberg, J., and Thieulot, C. 101 Geodynamic Modelling: How to Design, Interpret, and Communicate Numerical Studies of the Solid Earth. *Solid Earth*, 13(3):583–637, 2022. doi: 10.5194/se-13-583-2022.

Walton, M. A. L., Staisch, L. M., Dura, T., Pearl, J. K., Sherrod, B., Gomberg, J., Engelhart, S., Tréhu, A., Watt, J., Perkins, J., Witter, R. C., Bartlow, N., Goldfinger, C., Kelsey, H., Morey, A. E., Sahakian, V. J., Tobin, H., Wang, K., Wells, R., and Wirth, E. Toward an Integrative Geological and Geophysical View of Cascadia Subduction Zone Earthquakes. *Annual Review of Earth and Planetary Sciences*, 49(Volume 49, 2021):367–398, 2021. doi: 10.1146/annurev-earth-071620-065605.

Wendt, J., Oglesby, D. D., and Geist, E. L. Tsunamis and Splay Fault Dynamics. *Geophysical Research Letters*, 36(15), 2009. doi: 10.1029/2009GL038295.

Wilkinson, M. D., Dumontier, M., Aalbersberg, I. J., Appleton, G., Axton, M., Baak, A., Blomberg, N., Boiten, J.-W., da Silva Santos, L. B., Bourne, P. E., Bouwman, J., Brookes, A. J., Clark, T., Crosas, M., Dillo, I., Dumon, O., Edmunds, S., Evelo, C. T., Finkers, R., Gonzalez-Beltran, A., Gray, A. J. G., Groth, P., Goble, C., Grethe, J. S., Heringa, J., 't Hoen, P. A. C., Hooft, R., Kuhn, T., Kok, R., Kok, J., Lusher, S. J., Martone, M. E., Mons, A., Packer, A. L., Persson, B., Rocca-Serra, P., Roos, M., van Schaik, R., Sansone, S.-A., Schultes, E., Sengstag, T., Slater, T., Strawn, G., Swertz, M. A., Thompson, M., van der Lei, J., van Mulligen, E., Velterop, J., Waagmeester, A., Wittenburg, P., Wolstencroft, K., Zhao, J., and Mons, B. The FAIR Guiding Principles for Scientific Data Management and Stewardship. *Scientific Data*, 3(1):160018, 2016. doi: 10.1038/sdata.2016.18.

Williamson, A., Melgar, D., and Rim, D. The Effect of Earthquake Kinematics on Tsunami Propagation. *Journal of Geophysical Research: Solid Earth*, 124(11):11639–11650, 2019. doi: 10.1029/2019JB017522.

Wilson, A. and Ma, S. Wedge Plasticity and Fully Coupled Simulations of Dynamic Rupture and Tsunami in the Cascadia Subduction Zone. *Journal of Geophysical Research: Solid Earth*, 126(7): e2020JB021627, 2021. doi: 10.1029/2020JB021627.

Wirth, E. A., Sahakian, V. J., Wallace, L. M., and Melnick, D. The Occurrence and Hazards of Great Subduction Zone Earthquakes. *Nature Reviews Earth & Environment*, 3(2):125–140, 2022. doi: 10.1038/s43017-021-00245-w.

Zhang, W., Liu, Y., and Chen, X. A Mixed-Flux-Based Nodal Discontinuous Galerkin Method for 3D Dynamic Rupture Modeling. *Journal of Geophysical Research: Solid Earth*, 128(6): e2022JB025817, 2023. doi: 10.1029/2022JB025817.